ELECTRONIC SUPPLEMENTARY INFORMATION

Different catalytic behavior of amorphous and crystalline cobalt tungstate for electrochemical water oxidation

Hongfei Jia,*[a] Jason Stark,[a] Li Qin Zhou,[a] Chen Ling,[a] Takeshi Sekito,[b] Zachary Markin[a]

[a] Materials Research Department, Toyota Research Institute of North America, 1555 Woodridge Ave., Ann Arbor, MI 48105, USA

[b] Advanced Material Engineering Division, Toyota Motor Corporation, 1200, Mishuku, Susono, Shizuoka 410-1193, Japan

E-mail: hongfei.jia@tema.toyota.com

1. Details of experimental procedures

1.1 Synthesis of amorphous and crystalline $CoWO_4$ particles

Cobalt tungstate ($CoWO_4$) was synthesized by solution precipitation method. Cobalt nitrate hexahydrate $Co(NO_3)_2{\cdot}6H_2O$ (Sigma-Aldrich, ≥99.0%) and sodium tungstate dihydrate $Na_2WO_4{\cdot}2H_2O$ (Sigma-Aldrich, ≥99.0%) were first dissolved in 50 ml of distilled water separately at a concentration of 0.5 M. Then, Na_2WO_4 was slowly added to the $Co(NO_3)_2$ solution under vigorous stirring. Formation of purple precipitates was immediately observed upon addition of Na_2WO_4. The resultant slurry was rinsed with deionized water for at least 5 times on a centrifuge, followed by drying overnight in a vacuum oven (35°C) and in a tube furnace (under Ar) at 100°C for 5 hrs. The particles were subsequently heat-treated at elevated temperatures ranging from 200 to 500 °C (with 50°C intervals).

1.2 Materials properties XRD and XPS analysis

Powder X-ray diffraction patterns were obtained on a Rigaku Smartlab X-ray diffractometer using Cu Kα radiation (λ = 1.5405 Å). Data was collected in Bragg-Brettano mode using a scan rate of 1°/min. X-ray photoelectron spectroscopy (XPS) analysis was performed with a Kratos AXIS Ultra XPS using a monochromatized Al source that gives an energy resolution better than 0.5 eV when a pass energy smaller than 20 eV used. An ultra high vacuum ($<5\times10^{-9}$ Torr) was maintained for the measurement. Both survey scan (with 160 eV pass energy at a scan step of 1 eV) and high resolution (Co 2p), (W 4f), and (O 1s) scans (with 20 eV pass energy at a scan step of 0.1 eV) were performed. Carbon 1s peak (284.5 eV) from contamination was used to calibrate the spectra.

1.3 SEM/EDS and TEM

FEI Nova Nanolab 200 equipped with a EDXA X-ray energy-dispersive spectroscopy (EDS) system was used to characterize the surface morphology of the $CoWO_4$ samples and to identify the elements within the material. The acquisition time for EDS was 90-150 seconds. Quantitative element analysis of cobalt and tungsten were performed by integrating the EDS spectra. JEOL 3011 HRTEM was used for the study of the microstructures of the particles.

1.4 Diffusive reflectance spectroscopy

Diffuse reflectance was measured on a Lambda 1050 UV-Vis-NIR spectrophotometer using 150-mm integrating sphere (PerkinElmer, Inc.). Amorphous and crystalline $CoWO_4$ powders were loaded into a powder sample holder (PerkinElmer, Inc.) and clamped on the external port of the integrating sphere. The spectra were recorded in absorbance vs. wavelength mode.

1.5 Fabrication of composite catalyst thin film on glassy carbon electrode

Composite catalyst thin film preparation consisted of suspended $CoWO_4$ nanoparticles in a catalyst ink solution, which was deposited or "drop-cast" with 10μL pipette onto the surface of a glassy carbon (GC) electrode (0.196 cm^2 area, Pine, NC). Catalyst ink solutions were prepared as a liquid mixture consisting of five times the catalyst mass ratio to carbon black (CB) and to Nafion® (i.e. catalyst:CB: Nafion® = 5:1:1). The commercial stock of 5 wt % Nafion® (DE520, Ion Power, DE) required a 2:1 ratio of Nafion® to 0.1 M NaOH in order to stabilize its ion-exchange contribution in situ. The non-catalyst mass contributions in the catalyst ink solution were prepared with mixture of Nafion® solution (Nafion® + NaOH), tetrahydrofuran (THF, 99.9 +% Sigma-Aldrich), and CB pretreated with nitric acid overnight at 80°C. The catalyst was then added to complete the catalyst ink solution of which its solid nanoparticles could be suspended uniformly via iced-bath sonication followed by vortex mixing. The concentration consistency was maintained by immediately depositing the catalyst ink before particles settled out of momentary liquid suspension. The catalyst film was allowed to dry at room temperature in a sealed container for six of more hours and the final composition of the film was estimated to be 250, 50 and 50 μg/cm^2 for $CoWO_4$, CB and Nafion®, respectively.

1.6 Electrochemical analysis using rotating disk electrode

Electrochemical analysis was performed using either a Solartron 1287 Potentiostat/Galvanostat or a BioLogic VSP Electrochemical Work Station. Rotating disk electrode measurements were conducted using Pine Instruments MSR rotator attached to a glassy carbon disk electrode mounted inside an insolated head submerged in electrolyte within an electrochemical cell (**Figure S1 (a)**). An Ag/AgCl electrode (3M NaCl, 0.21 V vs. NHE) and a Pt coil (in fitted glass tube) were used as the reference and counter electrodes, respectively. In all tests, the cell was filled with 125 ml 0.2 M $NaWO_4$ electrolyte solution, of which the pH was adjusted with NaOH or HNO_3 solution. Prior to each test, the electrolyte solution was first purge with O_2 (ultra-high-grade purity, Airgas) for 15 min. After purging, O_2 flow was maintained in the headspace.

Cyclic voltammetry (CV) analysis was typically conducted at a scan rate of 15 mV/sec over an applied potential range of 0.66 to 1.46 V (NHE). All experiments started with a forward scan (potential low to high) and completed with a backward scan (potential high to low). For CV in Fig. 3, the potential range for crystalline $CoWO_4$ catalyst films and the control electrode were shifted to 0.76 V to 1.63 V to aid in graphical representation of their comparable performance.

Polarization behavior of the catalysts on rotating disk electrodes was investigated using both potentiostatic (constant potential) and galvanostatic (constant current) sweeps. The results for both studies correlate well with a high degree of repeatability, but in this article only the potentiostatic data were used to construct Tafel plots. Specifically, steady-state currents at applied potentials ascending from 1.01 to 1.26 V were recorded at ~ 25 mV per step. For applied potentials of 1.01 to 1.086 V, longer time (> 30 min) was required to reach the steady state. The internal resistances (IR) measured by impedance analysis were 53 and 39 **Ω** for amorphous and crystalline electrodes, respectively, which were compensated manually for the calculation of overpotentials. For each heat-treatment condition, three electrodes were prepared and tested in the same manner. Totally 21 samples were tested and the resulted Tafel plots with error bars are shown in **Figure S7**.

The pH dependence of $CoWO_4$ was investigated analogous to the method described in a previous literature (J. Am. Chem. Soc., **2010**, 132, 16501-16509), in which Co-Pi was investigated in a Co-free Pi electrolyte solution. The electrolyte pH was adjusted incremental by adding concentrated NaOH (40 %wt) or HNO_3 (35 %wt) to the electrolyte solution inside the electrochemical cell. Two experiments were performed, one measuring potential while controlling applied current and the other vise-versa. Conditioning with 5 cycles of CV in a pH 8 electrolyte solution of 0.2 M $NaWO_4$ was always done prior to each test.

1.7 Preparation of $CoWO_4$ film on ITO electrode

ITO glass slides were purchased from Delta Technology (Loveland, CO) and they came in the dimensions of 10x38x1.1 mm. Proper cleaning of ITO glass slides prior to deposition of $CoWO_4$ is critical to obtain good quality of film. ITO glass slides were first sonicated in isopropyl alcohol (IPA) for 10 minutes, then rinsed with deionized water. Subsequently, grease and dirt were removed by soaking ITO glass slides in ammonium hydroxide solution (3ml of ammonium hydroxide and 12 ml of water) for 3 to 5 minutes. Then the glass slides were rinsed with deionized water for about 1 minute. The glass slides were blown dry with nitrogen gas and used immediately.

The deposition of $CoWO_4$ nanoparticles onto ITO glass slide was done using an automatic Nima Multi Vessel Dip Coater. Prior to the operation, as-synthesized $CoWO_4$ nanoparticles were first dispersed in 1-butanol at a concentration of 2.5 mg/ml under sonication (20 minutes) to form a stable suspension. Fairly uniform coatings were obtained after 100 repetitions and then baked in an oven at 150°C for an hour to remove the solvent. As-coated $CoWO_4$ films were amorphous. The films were subsequently heat-treated in argon at 500°C for an hour to reach crystallization. As the intention of using catalyst film on ITO is to qualitatively examine the difference between amorphous and crystalline catalyst, no special effort was made to control catalyst loading and optimize film quality. The effective area of the catalyst films on the working electrode was typically ~ 2 cm^2.

1.8 Faradaic efficiency measurement and calculation

Two types of samples were tested for Faradaic efficiency evaluation: as-coated amorphous and crystalline $CoWO_4$ films. The experiments were performed in a custom built gas-tight electrochemical cell, as illustrated in **Figure S1 (b)**. The chemical cell used pH 8 0.2 M Na_2WO_4 aqueous solution as the electrolyte, Ag/AgCl as reference electrode, and Pt coil as counter electrode. The cell was purged with Ar for 2 hours and then sealed before the test. A potential of 1.36 V (NHE) was applied to the electrodes for 45 minutes. Charge transfer data was recorded along with oxygen production measured using a fluorescence-based O_2 sensor (Ocean Optics, FOXY-R). Faradaic efficiency was determined through comparison of the calculated theoretical O_2 production based on recorded charge transfer to the actual O_2 production detected. Actual O_2 production included both the O_2 in the headspace, found via the sensor, and the O_2 dissolved in electrolyte estimated according to the Henry's law.

2. Additional Figures and Tables

Figure S1. Electrochemical cell setups for rotating disk electrodes and bulk electrolysis experiments

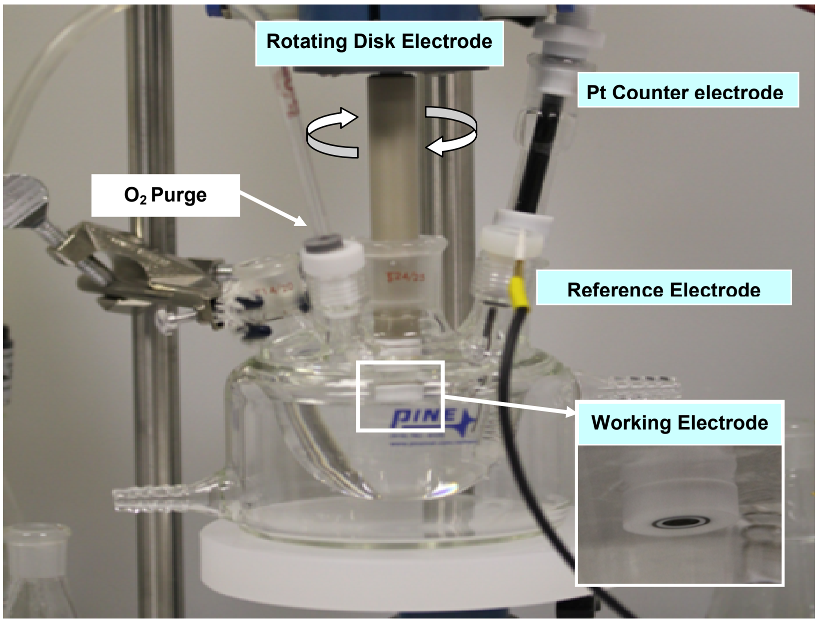

(a) Electrochemical cell used for tests with rotating disk electrodes

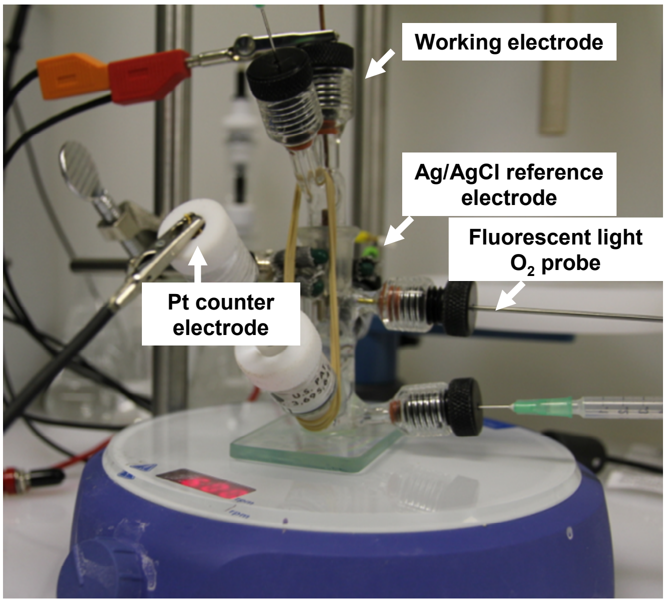

(b) Electrochemical cell used for bulk electrolysis and Faraday efficiency estimation

Figure S2. pH Titration of Na_2WO_4 with HNO_3

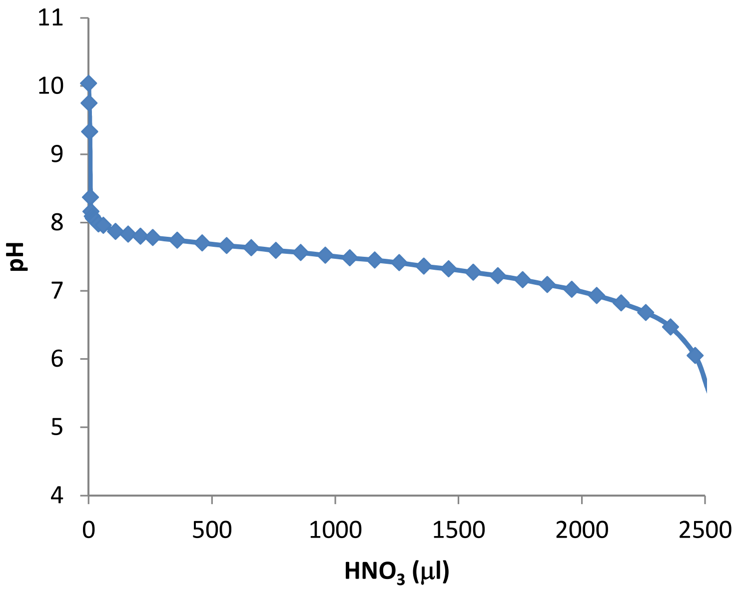

The titration was done by adding small volumes of concentrated HNO_3 (5 M) to 50 ml of Na_2WO_4 (0.2 M) solution while monitoring the pH change.

Figure S3. XRD spectrum of crystalline $CoWO_4$ with peak indexing information

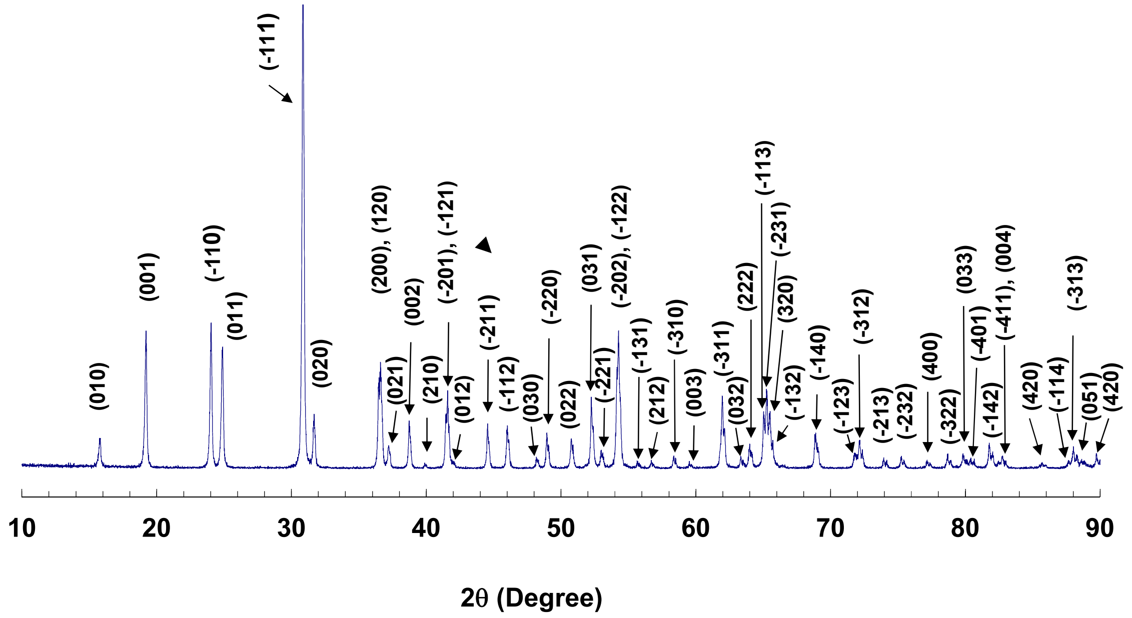

Figure S4. BET specific surface area determined by nitrogen adsorption/desorption

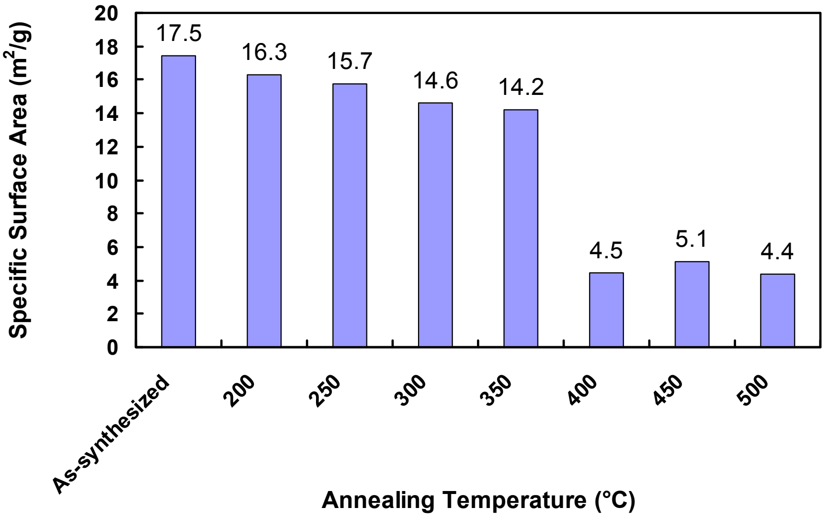

Specific surface areas of $CoWO_4$ nanoparticles annealed at different temperatures were measured via BET analysis by Particle Technology Labs (Downers Grove, IL). As shown above, the specific surface area decreases as the annealing temperature increases. A clear drop in specific surface area occurred at 400°C, in good alignment with the XRD results (**Fig. 1**) where a structural transition from amorphous to crystalline appeared at 400°C as well.

Figure S5. Optical absorption spectra of amorphous and crystalline $CoWO_4$

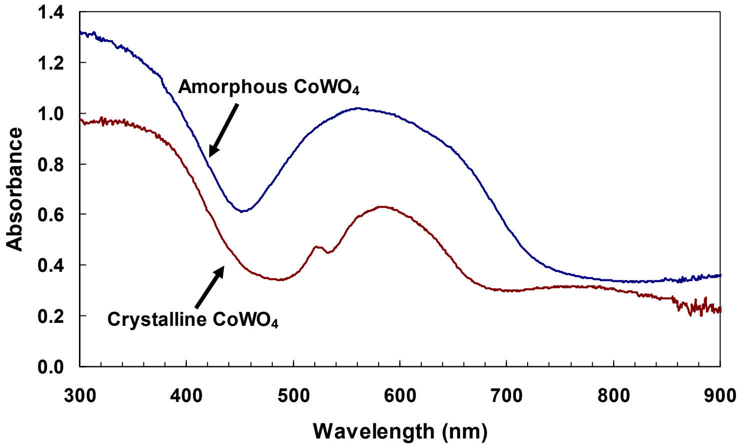

Both the amorphous (as-synthesized) and the crystalline (heat treated at 500°C for 1 hour) $CoWO_4$ powders show two strong cut-offs at around 450-400 nm and 750-700 nm, which indicate two possible optical band gaps.

Figure S6. Cyclic voltammogram of crystalline $CoWO_4$ electrode

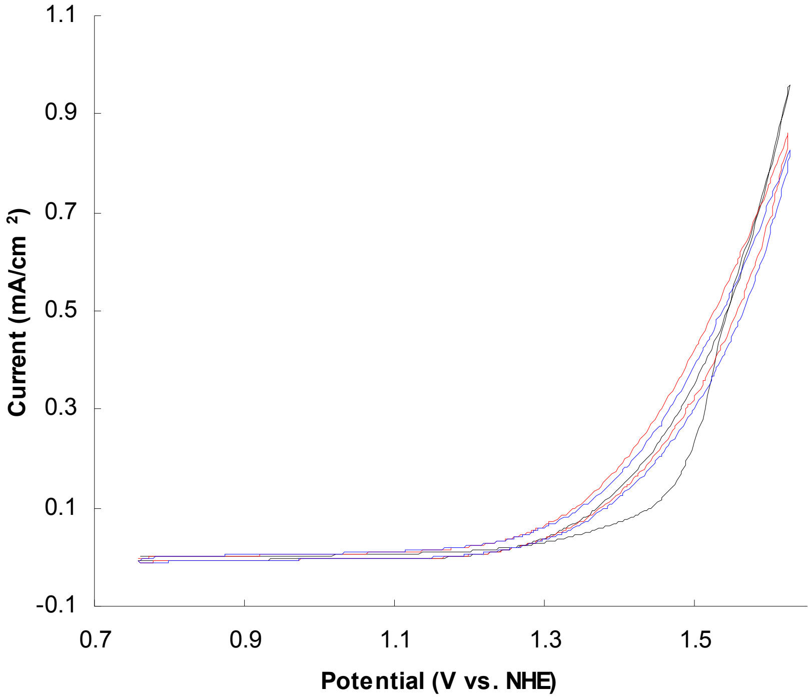

Cyclic voltammograms were obtained from glassy carbon electrodes coated with carbon black, Nafion® and crystalline $CoWO_4$ (treated at 500°C). Black, red and blue lines denote to the first, second and third scans, respectively. Scan rate: 15 mV/s.

Figure S7. Complete Tafel plots with error bars

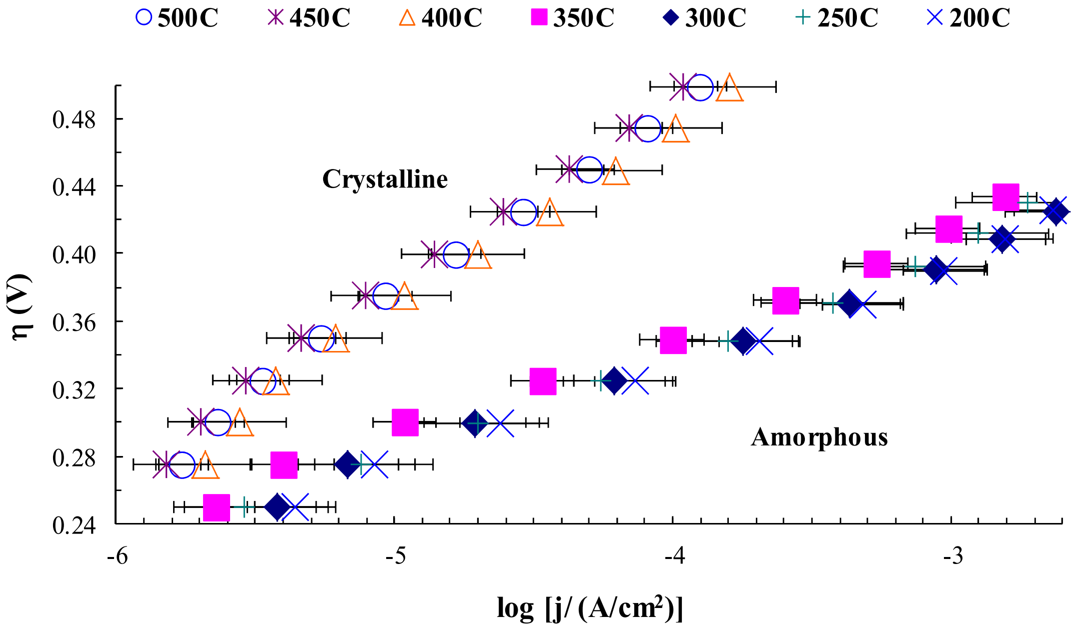

Figure S8. Faraday efficiency as determined via bulk electrolysis

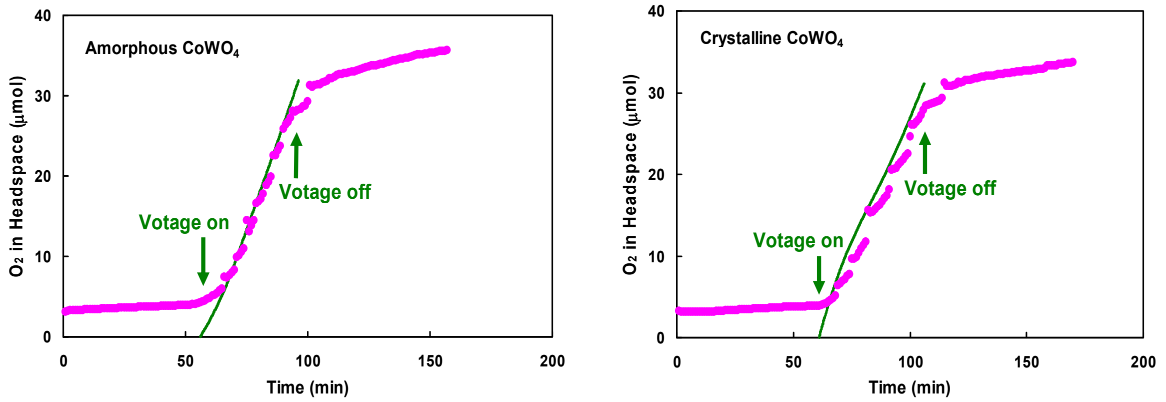

Faraday efficiency is estimated by comparing the theoretical (green) and actually observed (pink) O_2 production in the headspace over the amorphous (left) and the crystalline (right) $CoWO_4$ electrode. Theoretical O_2 production was calculated based on the recorded charge transfer and assumption of $4e^-$ oxidation of water. Actual O_2 production included both the O_2 recorded in the headspace via the sensor and the O_2 dissolved in electrolyte estimated according to the Henry's law. The amount of O_2 detected in the headspace increased in accordance with the theoretical prediction. The estimated Faraday efficiencies were found to be relatively similar at ~90% for both amorphous and crystalline $CoWO_4$ films.

Figure S9. XPS survey spectrum of as-synthesized $CoWO_4$

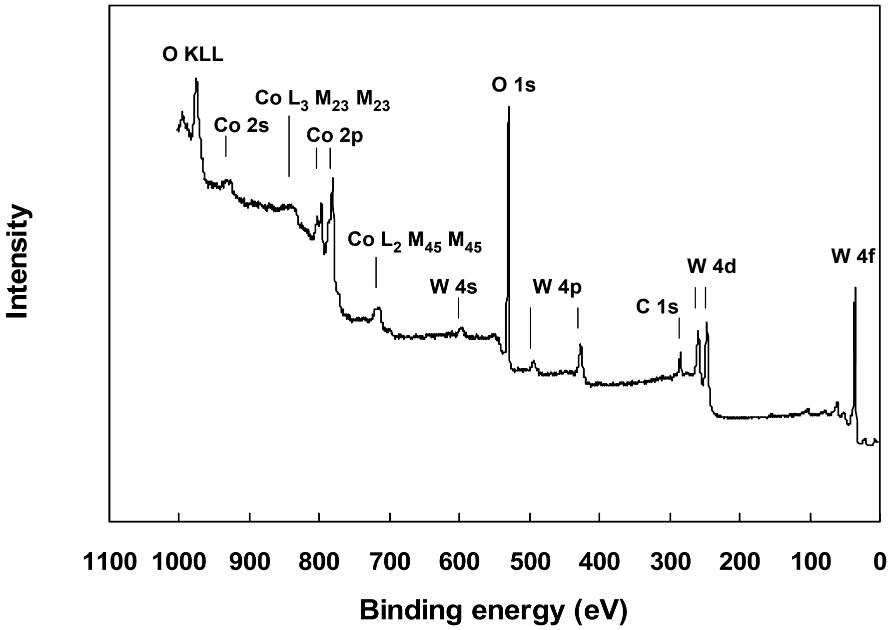

All the spectral features of the survey spectrum, except for the C 1s level (from impurities), are attributed to the constituent element core-levels or Auger lines. Survey XPS spectra of amorphous and crystalline $CoWO_4$ film before and after being used for catalyzing water oxidation reaction showed very similar patterns to that of as-synthesized nanoparticles, thus not shown here. However, high resolution scans, particularly Co 2p peaks exhibited significant differences. The details are discussed in the main article (**Fig. 6**).

Figure S10. SEM images of amorphous and crystalline $CoWO_4$-ITO electrodes

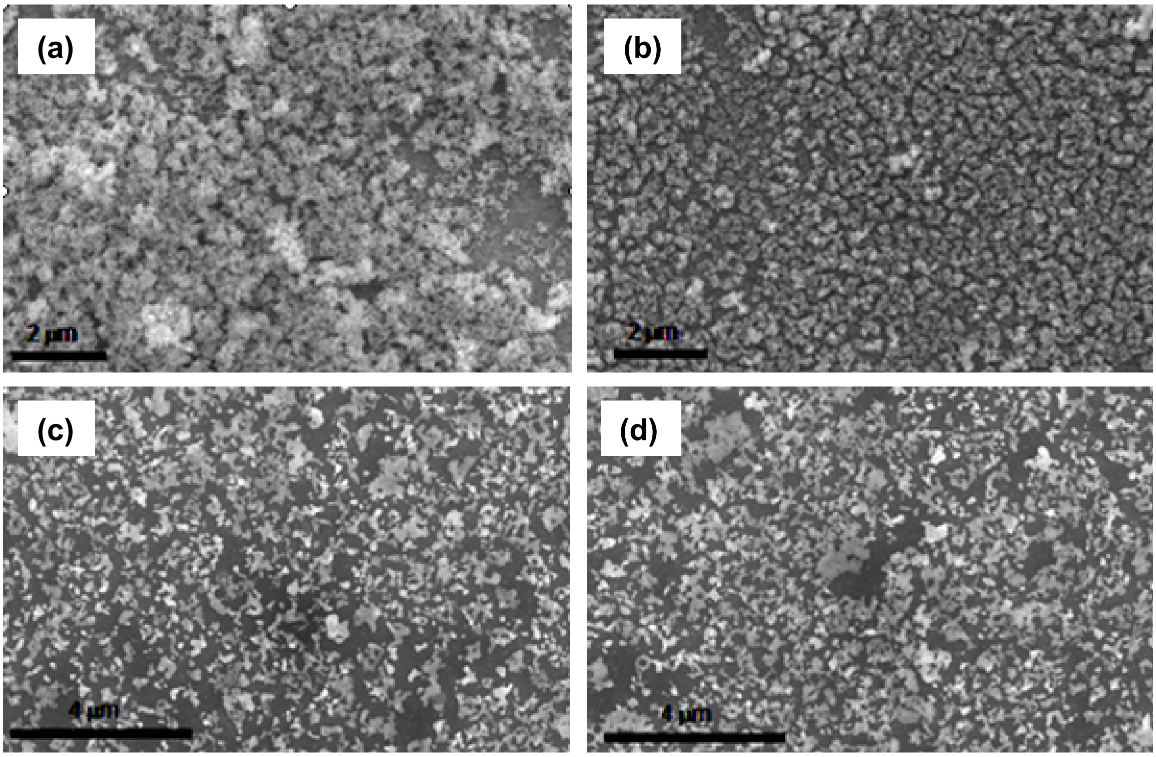

SEM images above show the morphology of dip-coated $CoWO_4$ on ITO electrodes before and after multiple CV scans and bulk electrolysis: (a) fresh amorphous, (b) used amorphous (c) fresh crystalline and (d) used crystalline. For the amorphous $CoWO_4$, a more densely compacted morphology was seen after the usage. While for the crystalline $CoWO_4$, no evident change on morphology was observed.

Table S1. Results of EDS analysis of amorphous and crystalline $CoWO_4$-ITO electrodes

Quantitative element analysis was conduced to estimate the ratio of cobalt to tungsten. Average chemical compositions (ratio of Co to W) of the amorphous and the crystalline $CoWO_4$ on ITO were calculated based on ten EDS spectra for each sample.

Sample	Electrochemical Cycling	Atomic ratio of Co to W
Amorphous $CoWO_4$	Before	0.85 ± 0.03
	After	0.91± 0.02
Crystalline $CoWO_4$	Before	0.86 ± 0.04
	After	0.84 ± 0.06